MCMC Shape Sampling for Image Segmentation with Nonparametric Shape Priors

Supplementary Material

1. Experiments on the aircraft data set

As we mentioned in the paper, the aircraft data set contains 11 synthetically generated binary aircraft images and the test images are constructed cropping the left wings from the binary images to simulate occlusion and by adding some noise. We constructed two different test image sets: one has higher SNR (test image set - 1) compared to the other (test image set - 2). In the paper, we presented the results on three test images for each image set. In this supplementary material, we provide results on the remaining 8 test images for both test image set - 1 (see Figure 1) and test image set - 2 (see Figure 2).

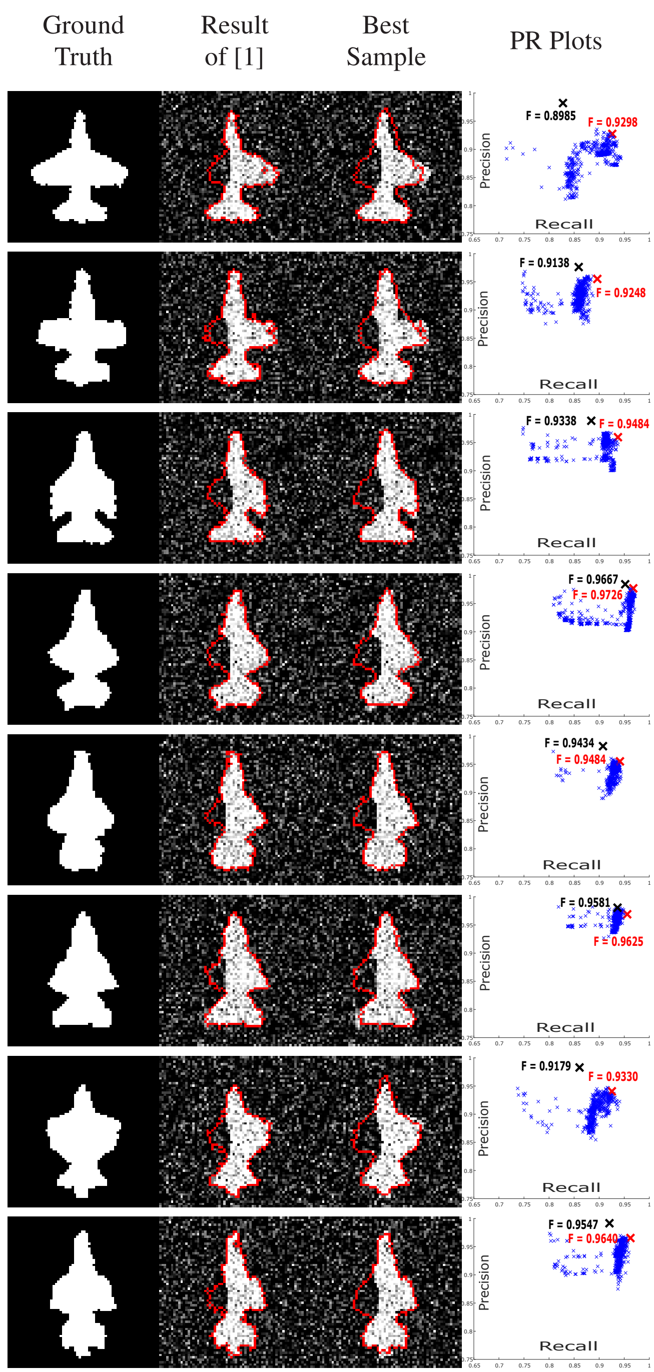

Figure 1. Experiments on test image set - 1 of the aircraft data set. Note that each row contains the results for a different test image. In the PR plots, ‘×’and ‘×’mark the samples produced by our approach where ‘×’indicates the sample with the best F-measure value, and ‘×’marks that of segmentation of Kim et al. [1].

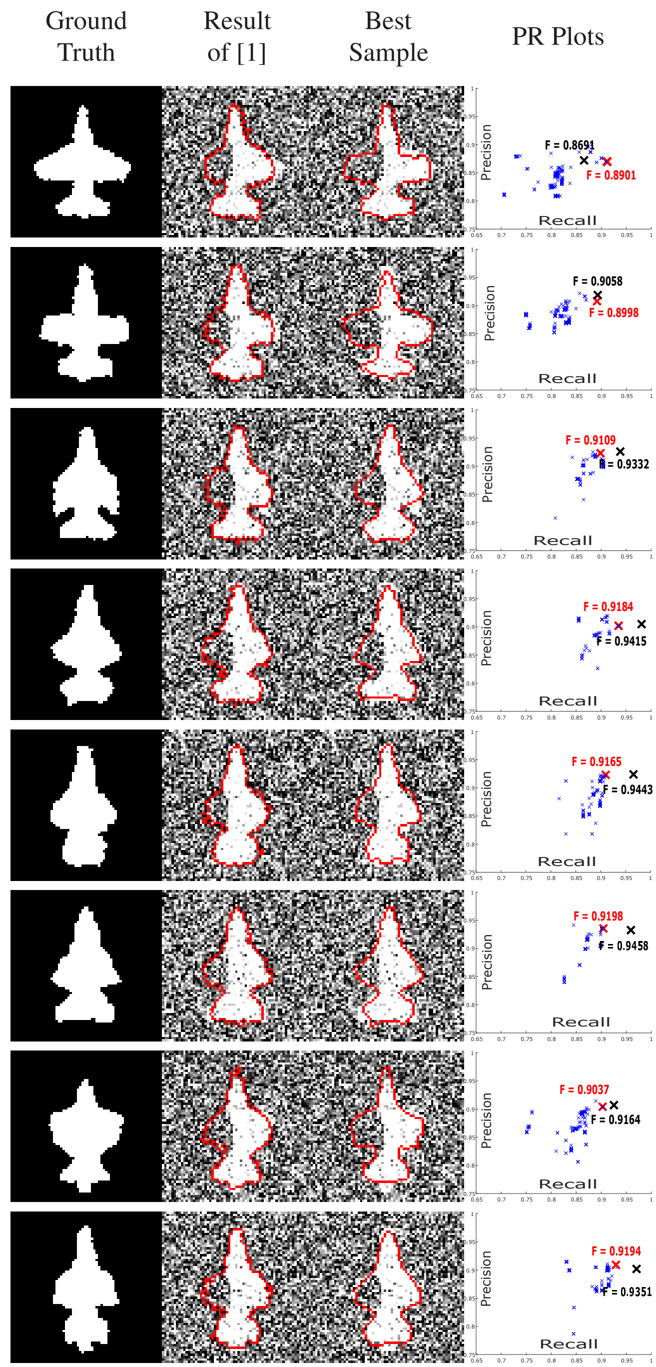

Figure 2. Experiments on test image set - 2 of the aircraft data set. Note that each row contains the results for a different test image. In the PR plots, '$\times$'and '$\times$'mark the samples produced by our approach where '$\times$'indicates the sample with the best F-measure value, and '$\times$'marks that of segmentation of Kim et al. [1].

Note that, in the case of occlusion, we use $\pi(C) \propto \exp(-E_{shape}(C))$ instead of $\pi(C) \propto \exp(-E(C))$ as we explained in Section 6 in the main paper. However, if we have information about the location of the missing pixels we can use $\pi(C) \propto \exp(-E(C))$ since we do not take into the account pixels in the missing region when computing $E_{data}(C)$. We also perform some experiments in the case of missing data to show that our approach is able to generate samples from the posterior. These results can be seen in Figure 3.

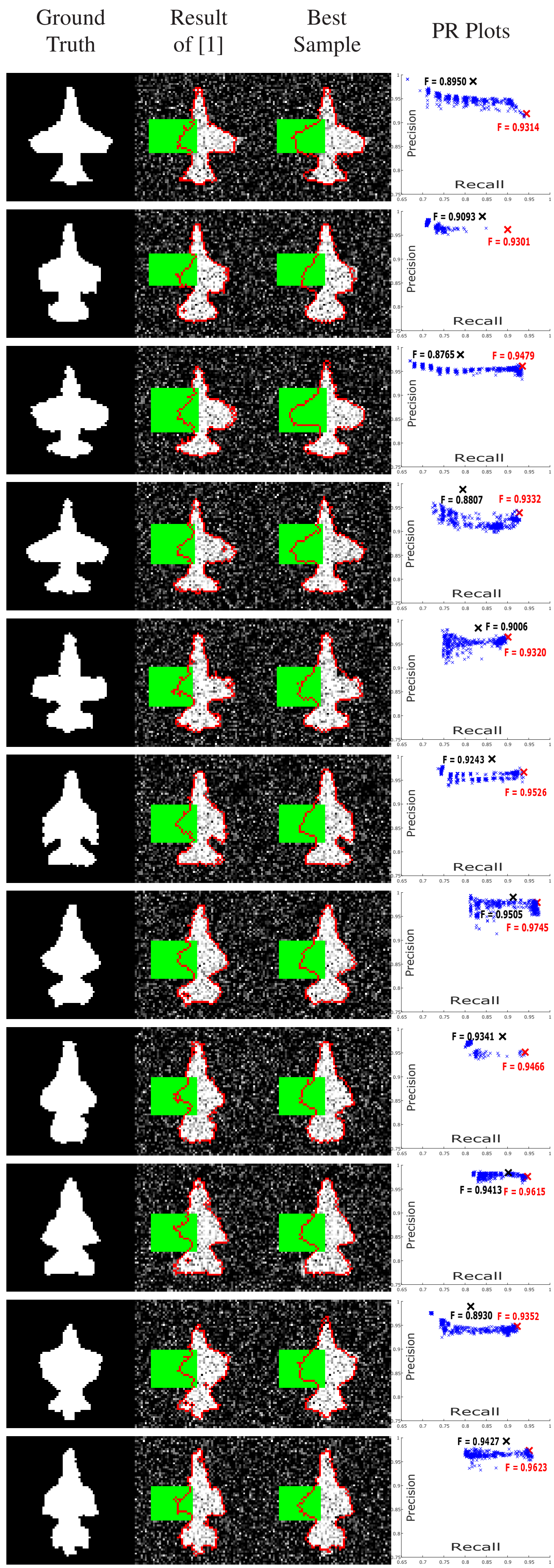

Figure 3. Experiments on test image set - 1 of the aircraft data set in a scenario where we know missing pixels (shown by green). Note that each row contains the results for a different test image. In the PR plots, '×'and '×'mark the samples produced by our approach where '×'indicates the sample with the best F-measure value, and '×'marks that of segmentation of Kim et al. [1].

2. Experiments on the MNIST data set

We have performed experiments on three different test images (MNIST - 1, MNIST - 2, and MNIST - 3) from the MNIST data set. In this supplementary material, we present samples from the best 5 classes including the best 3 classes presented in the paper (see Figure 5).

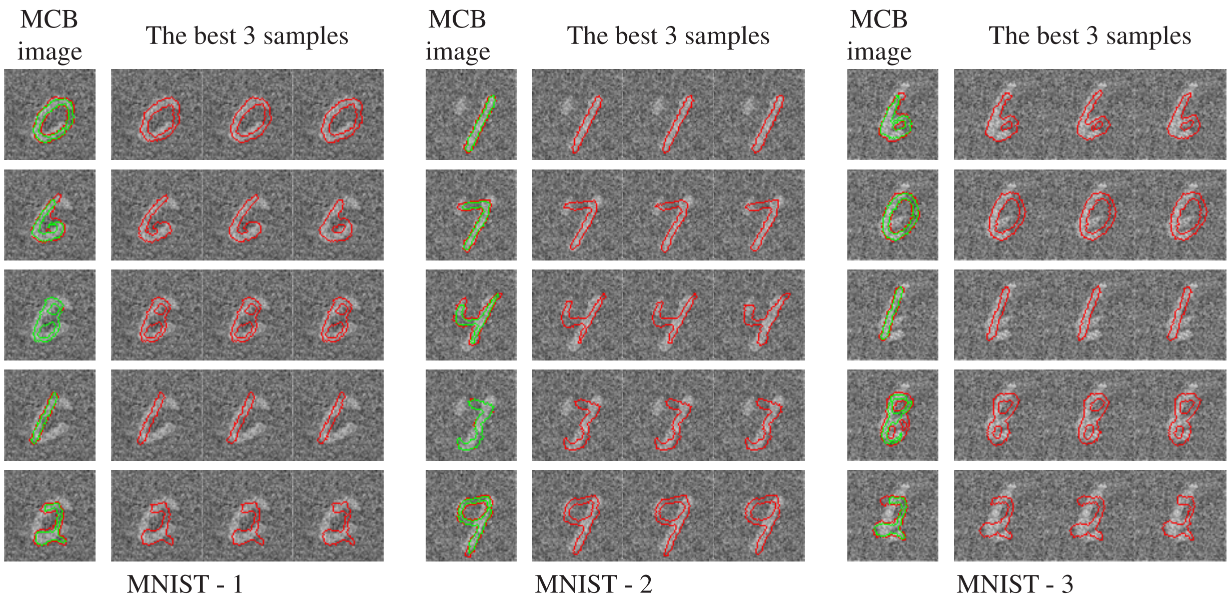

Figure 4. Experiments on the MNIST data set. Note that the images in the first column of the results for each test image indicate the marginal confidence bounds (MCB image), where red and yellow contours are the marginal confidence bounds at $H(x) = 0.1$ and $H(x) = 0.9$, respectively.

3. Experiments on the walking silhouettes data set

The walking silhouettes data set contains 14 test images and the results of the first three test images with both global and local shape priors are shown in the paper. In this supplementary material, we present results on the remaining 11 test images in Figure 5.

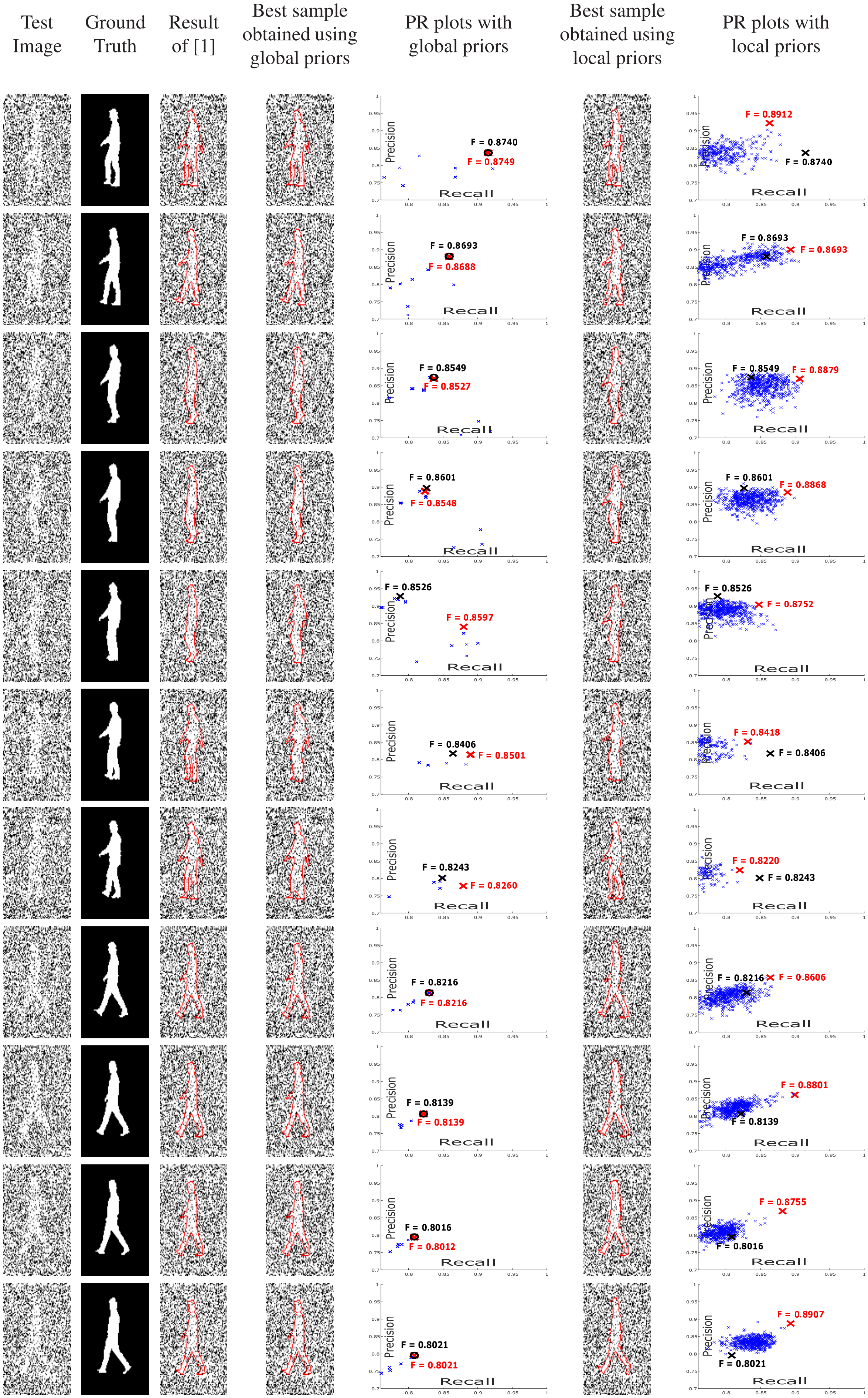

Figure 5. Experiments on the walking silhouettes data set. In the PR curves, the '×'marks the sample having the best F-measure value obtained using the proposed approach (with either global or local shape priors), and the '×'marks that of segmentation of Kim et al. [1].

References

[1] J. Kim, M. Çetin, and A. S. Willsky. Nonparametric shape priors for active contour-based image segmentation. *Signal Processing*, 87(12):3021–3044, 2007.